Asian Journal of Engineering Geology, 2025, Vol. 2 No. 2, 29-40

Research Article DOI: https://doi.org/10.64862/ajeg.2025.202.04.301 Open Access

SWAT-Based Hydrological Modeling and Water Balance Dynamics of West Rapti River Basin, Nepal

Rabindra Bahadur Thapa[1], Kumud Raj Kafle[2*] and Kundan Lal Shrestha[3]

[1]Department of Water Resources and Irrigation, Jawalakhel, Lalitpur, Nepal
[2]Department of Environmental Science and Engineering, Kathmandu University, Dhulikhel, Nepal
[3]Department of Chemical Engineering, Kathmandu University, Dhulikhel, Nepal

([*]Corresponding E-mail: krkafle@ku.edu.np)

Received: June 04, 2025, Accepted: December 15, 2025

Abstract: This study simulated the hydrological and sediment dynamics of Nepal's West Rapti River Basin (WRB) using the Soil and Water Assessment Tool (SWAT) to quantify water balance components and sediment yield. The model integrated a 30 m resolution digital elevation model (DEM), soil maps, and land use data, delineating the basin into 21 sub-basins and 180 hydrological response units (HRUs). Sensitivity analysis identified the curve number (CN2), baseflow recession coefficient (ALFA_BF), and surface runoff lag time (SURLAG) as the most influential hydrological parameters. The SWAT model was calibrated (2003–2011) and validated (2012–2020) using observed discharge at Jalkundi station. The model showed strong performance, with coefficient of determination (R^2) values of 0.95 and 0.91 and Nash–Sutcliffe efficiency (NSE) values of 0.76 and 0.75 during calibration and validation, respectively. Percent bias (PBIAS) ranged from −7.7% to −13.5%, indicating slight overestimation of baseflow. Sediment simulation achieved R^2 and NSE values of approximately 0.60, representing satisfactory performance. Long-term simulation (2000–2022) estimated a mean annual precipitation of 1,676 mm, with about 55% contributing to streamflow, resulting in an average annual water yield of 951 mm, while 42% was lost through evapotranspiration. Surface runoff averaged 573 mm yr^{-1} and peaked during the monsoon season. Mean annual sediment yield was 166 t ha^{-1} yr^{-1}, varying from 15.68 to 468.05 t ha^{-1} yr^{-1} across sub-basins. Sub-basin 8 recorded the highest sediment yield because of steep slopes (>40%) and erosive land use. Approximately 68% of annual streamflow and 85% of sediment yield occurred during the monsoon (June–September). These findings demonstrate the capability of the SWAT model to support watershed management, sediment control, and sustainable water resource planning in the WRB.

Keywords*: Hydrology, SWAT, Water balance, Model performance, Model calibration, Model validation*.

Introduction

River basins are key ecosystems for the sustenance of human civilization by providing basic resources to millions of people, among them indigenous ethnic minorities who directly depend on these ecosystems for their livelihood (Bohara et al., 2025). A river basin can be understood as the whole surface area drained by a river and its feeders, sustaining both ecosystems and human populations, with an accentuation on indigenous communities within its benefits. Hydrologically, river basins play the most crucial role in regulating water availability for agriculture and infrastructure (Basnet et al, 2024). The pressure on water resources, accompanied by changes in the hydrological cycle and degradation of basin ecosystems due to rapid development and population increase, was articulated by the UN in 2016. Inappropriate land use, deforestation activities, and climatic variations have disturbed natural dynamics related to water balance components both at upstream and downstream areas (Moges and Bhat, 2020). Precipitation partitioning into surface runoff, evapotranspiration, and groundwater recharge defines the hydrological resilience of a basin since it takes place within it. Anthropogenic activities like building dams and diverting rivers, which change flow regimes, call for strong hydrological modeling to assess such impacts (Owens, 2020; de Oliveira Serrão et al., 2022).

Hydrological simulation, together with the analysis of the water balance, forms the core element in sensitivity studies of the impacts of land use and climate variability on water resources within river basins (Nepal et al., 2024; Thapa et al., 2005). Changes in infiltration, surface runoff, and recharge of groundwater induced by urbanization or intensified agriculture directly control hydrological response at the basin scale (Ren et al., 2021). Accurate quantification of these dynamics is a prerequisite for modeling approaches applicable to simulate fluxes and storage variations involved in available water resource management. Possible imbalances caused by altered precipitation patterns or increased irrigation demand will also challenge the existing components' water security (Vercruysse et al., 2017). An assessment that would fully document the hydrological processes that take place in streamflow variation and seasonal water budgets (Van Oost et al., 2002).

Combining physical hydrological models with geospatial data has made a comprehensive understanding of the impact catchment-scale transformations, such as afforestation or urbanization, have on water cycling and nutrient transport possible (Schweizer et al., 2018; Pant et al., 2025). Land Use Change simulation or climate projections provide

potential impacts on river discharge and groundwater recharge as well as ecosystem stability, for scientifically informed policy decisions. Advancements in the Geographic Information System and hydrological modeling brought dramatic improvements to water balance evaluations through accurate simulations of complex hydrological processes (Liu and Jiang, 2019; Bishwakarma et al., 2024). The Soil and Water Assessment (SWAT) model is known to be one of the best physically based models used for simulating surface and subsurface runoff generation mechanisms with accompanying soil moisture variations and actual evapotranspiration components at various spatial and temporal scales (Ayele et al., 2021; Bekele and Abate, 2020; Subedi et al.,2024). By using climate data, land-use maps, and soil features as input, SWAT provides reliable predictions of water resources in ungauged basins to support the assessment of management options, for example, the optimization of irrigation or afforestation (Toma et al., 2023). As observed by Rahman et al. (2024) and Sinha et al. (2019), remote sensing is also found to contribute towards these through providing spatial detail information on precipitation and evapotranspiration that goes into better model performance, and also real-time tracking of hydrological changes at the basin scale. When used together with climate and land use scenarios, SWAT has been found effective in making forecasts of future vulnerabilities in water resources, thus informing adaptive management strategies in regions highly pressured climatically, such as those identified by Chilagane et al. (2021) and Li et al. (2022).

In the West Rapti River Basin, climate projections for South Asia indicate erratic monsoon and rising temperatures, posing significant threats to streamflow trend, intensifying drought risks, and reducing groundwater recharge (Shi et al., 2018). These challenges are further compounded by unsustainable practices such as deforestation and inefficient irrigation, which accelerate soil erosion and diminish the basin's capacity to retain water (Van Oost et al., 2002; Vercruysse et al., 2017). However, the localized hydrological effects of these combined climatic and human-induced pressures remain insufficiently quantified, limiting the effectiveness of targeted mitigation strategies. To address these gaps, this study utilizes the SWAT model to: (1) establish a baseline assessment of the basin's hydrological dynamics, including runoff, evapotranspiration, water yield, sediment yield, and groundwater recharge, and (2) analyze the basin's response to projected climate change scenarios. Establishing a baseline is crucial for identifying existing stressors, such as erosion-prone areas or inefficiencies in water allocation, while climate simulations (IPCC scenarios) will provide insights into shifts in streamflow seasonality, flood frequency, and aquifer behavior.

Methodology and materials

Description of the study area

The West Rapti River Basin is situated in the southwestern part of Nepal in Lumbini Province. It covers an area of approximately 6,380 km^2. Geographically, the basin extends between 27°45'10" N to 28°35'35" N and 81°40'10" E to 83°10'55" E. The length of the main river is 260 km from its origin to the basin outlet (Figure 1). The West Rapti River originates from the middle mountains region of Nepal and flows southward through rugged highlands into the lowlands, eventually draining into the Ghagra River in India. Jhimruk and Madi Rivers are two major tributaries of the west Rapti. Rainfall and groundwater are the primary contributors to its flow. The basin is characterized by its diverse topography, with elevations ranging from 70 m to 3,609 m above sea level (asl). The upstream portion of the basin exhibits a temperate climate, while the lower areas experience a tropical climate. The south region of the basin, primarily below 500 masl, consists of lowlands and accounts for approximately 34% of the total basin area. Geographically, the basin is wide in its headwaters and narrows toward the lower reaches. This has caused distinct variation in landscape and climate. The average annual precipitation for the basin is 1500 mm (Figure 2).

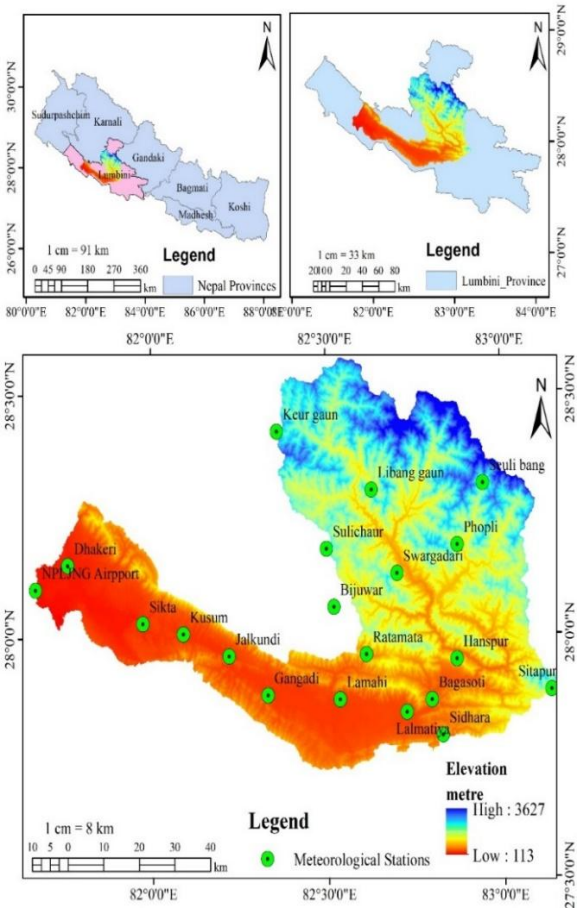

Figure 1, Map showing the study area of the Rapti River basin

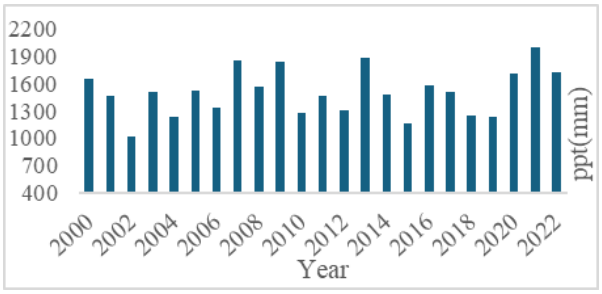

Figure 2, Average annual precipitation trend of the West Rapti River Basin

Data used

Different types of data are required to simulate the river basin hydrology using SWAT model. In this study, Digital Elevation Model (DEM), Land use/land cover, and Soil map are used as spatial data, the meteorological data, such as temperature and precipitation, have been used for this study. The Hargreaves method was used for the estimation of potential evapotranspiration (PET). Flow and sediment data obtained from the DHM Nepal are also used during the process of model calibration and validation.

Table 1, Sources of data used

S.N.	Data	Source	Type
1	DEM	ASTERGDEM website (https://gdemdl.aster.jspacesystems.or.jp/index_en.html)	Spatial grid
2	Soil Map	FAO (https://www.fao.org/soils-portal/data-hub/soil-maps-and-databases/harmonized-world-soil-database-v20/en/)	Spatial grid
3	LULC Map	ICIMOD (https://rds.icimod.org/DatasetMasters/Download/1972729)	Spatial grid
4	Precipitation and Temperature	Department of Hydrology and Meteorology, Nepal	Time series
5	River Flow and Sediment	Department of Hydrology and Meteorology, Nepal	Time series

Spatial data

Digital elevation model (DEM)

The DEM of 30-meter resolution was downloaded from the ASTER Global Digital Elevation Model website (Bhatta et al., 2019). The analysis of DEM shows that the elevation of the basin extends from 113 m to 3627 masl. The ASTER GDEM has good vertical accuracy for the root mean square error (RMSE) of 24 meters in Indian and Nepalese regions (Thomas et al., 2014). ASTER DEM could meet the demand in India and Nepal because it is accurate, easily obtainable, and suitable for the complex territorial structure of the Himalayas. With a resolution of 30 meters and a high level of vertical accuracy, ASTER DEM is capable of providing detailed information on the elevation, especially in regions with mountainous terrain, compared to other datasets such as SRTM (Thomas et al., 2014). This data set provides accurate topography information, which makes it useful in hydrology, sediment research, and disaster management. Free and easily accessible, ASTER DEM is a viable and cheaper option as compared to LiDAR data, for instance, making it easily accessible to researchers and policy makers in India and Nepal for applications in flood modeling, watershed management, and sustainable development (Shinde et al., 2013). These features make it a crucial application in environmental as well as scientific research in these areas. Further, the slope map was also derived from the DEM. During HRU analysis, multiple slope classes were designated as 0-5%, 5-15%, 15-25%, 25-40%, and more than 40%.

Land use land cover map

Land use/ land cover data in this study have been taken from the Forest Research Training Centre (FRTC) Nepal, with 30 m resolution (FRTC, 2022). The total LULC class classes were 8 among which the highest and lowest area covered by forest (69.61%) and barren land (0.001%) as shown in Figure 3.

Table 2, Land use land cover (LULC) data

SN	LULC type	Area %
1	Water	0.450
2	Forest	63.658
3	Riverbed	1.704
4	Built-up	0.220
5	Cropland	23.018
6	Barren	0.001
7	Rangeland	5.002
8	Woodland	5.947

Soil map

Soil map, along with soil data properties, was cited from the Food and Agriculture Organization (FAO). HWSD (Harmonized world soil data) was applied for soil properties classification (FAO, 2002). The map originally obtained in vector form was rasterized with pixel matching that of the DEM, i.e., 30 m resolution. Soil map of the basin has 4 soil types viz., I-Bh-U-c (lithic/rock debris), Bd34-2bc (stony), Rd30-2d, and Je75-2a, and as shown in Figure 3 and Table 3.

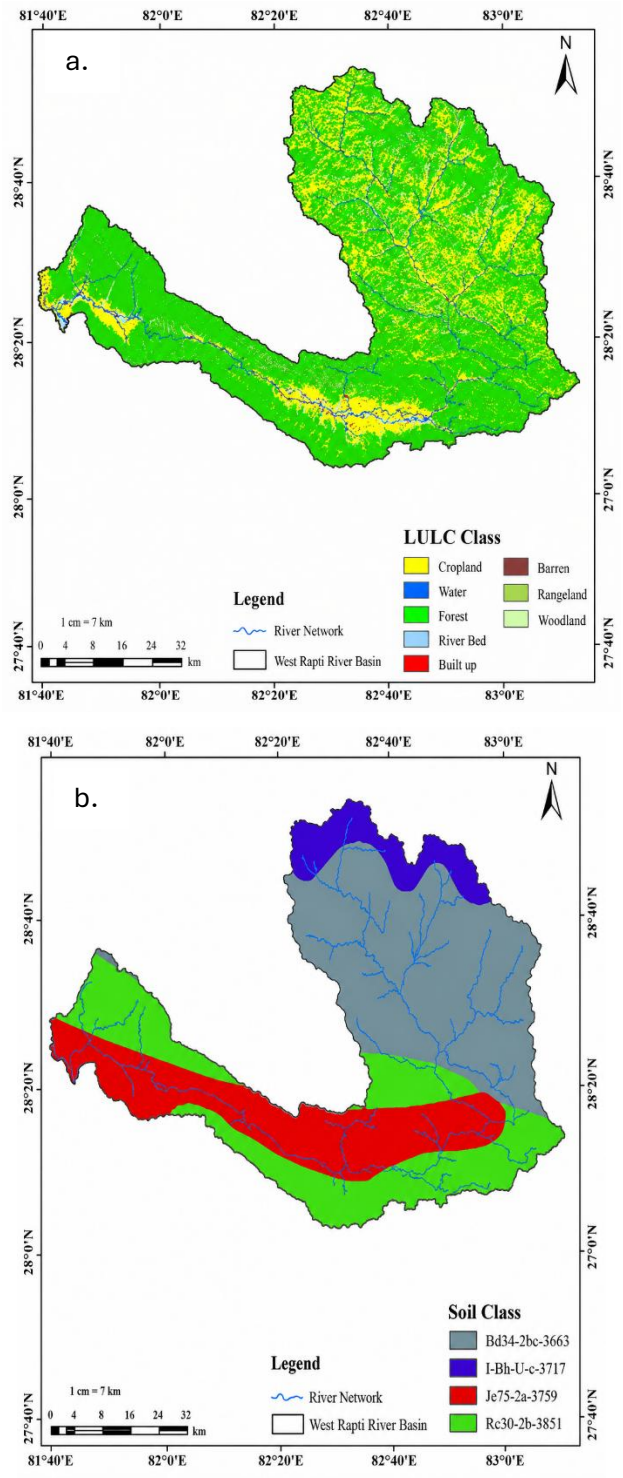

Figure 3, a. Land use land cover map and b. FAO soil map

Hydro-meteorological data

The daily observed meteorological data (maximum and minimum temperature, and average precipitation) for the basin were acquired from the Department of Hydrology and Meteorology (DHM) for 13 spatially distributed stations within the basin, covering the period from 2000 to 2022. Missing precipitation data were estimated using the Arithmetic Mean Method (Abdullah and Al-Ansari, 2022). Additionally, the simulation algorithm in the SWAT model was employed to derive the data for relative humidity, solar radiation, and wind speed across the river basin. The availability of high-resolution meteorological data is essential for accurately simulating hydrological processes such as runoff generation and water yield (Srivastava et al., 2020).

Table 3, FAO soil data

SN	Soil type	Area%
1	I-Bh-U-c	7.424
2	Bd34-2bc	42.020
3	Rd30-2b	26.994
4	Je75-2a	23.562

Observed monthly discharge data at Jalkundi station, which lies in sub-basin 18 as per the watershed delineation, was obtained from DHM for 2000 to 2022 to process flow calibration and validation of the model. Similarly, the monthly sediment concentration data for the Jalkundi station were obtained from the DHM for the calibration and validation of sediment in the model.

The Department of Hydrology and Meteorology provided historical sediment concentration data for the discharge measuring station Jalkundi (Station ID 360) since the most recent time series sediment for the river could not be located. Data on sediment concentration are dispersed. The 1985–1989 data is available. Using the available sediment load and outflow data from Jalkundi Station (Station 360), a sediment rating curve was created, and the sediment load, expressed in tonnes per day, was estimated. The developed rating curve, represented by a power equation, is given as S (tonnes/day) = 2.7081 × $Q^{1.5557}$, where S denotes the sediment load, and Q represents the daily discharge in cubic meters per second (m^3/s). The equation exhibited a correlation coefficient (R^2) of 0.65, indicating a moderate relationship between discharge and sediment load (Figure 4).

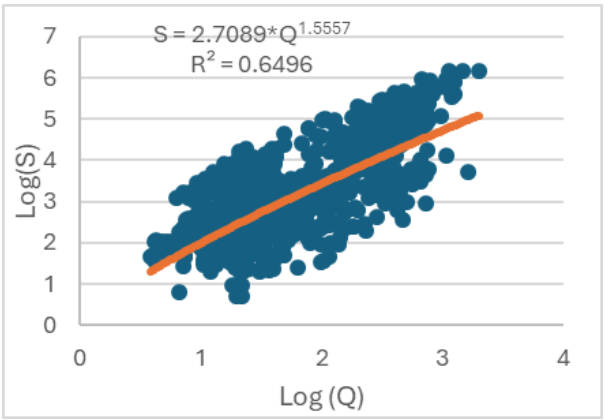

Figure 4, Sediment Rating Curve

Using the finalized sediment discharge rating equation, the sediment load (tonnes per day) was estimated. A daily data series was then generated, from which monthly sediment data were derived. This

dataset was subsequently utilized for the calibration and validation of the SWAT model.

Hydrological modeling of the west Rapti river basin

The SWAT model (Figure 5) was used for hydrological modeling of the West Rapti River basin (Figure 6). It is a semi-distributed, process-oriented, continuous-time watershed model created by the USDA to evaluate how different management strategies affect nonpoint source pollution and water resources in extensive catchment areas (Toma et al., 2023). The SWAT model deals with major components such as hydrology, vegetation growth, reservoir dynamics, land use management, pesticide behavior, and sediment transport in a river basin. The hydrological cycle of SWAT is governed by the following water balance equation (Arnold et al, 1998):

$$SWt = SW0 + \sum_{i=1}^{n}(Rday - Qsurf - Ea - Wseep - Qgw) \quad (1)$$

Where *SWt*: soil water content at time step t, *SW0*: initial soil water content, *Rday*: daily precipitation, *Qsurf*: runoff, *Ea*: evapotranspiration, *Wseep*: percolation and *Qgw*: groundwater flow.

Watershed delineation, HRU analysis, model set-up, and run

The SWAT initially delineates the watershed and further subdivides it into smaller sub-basins based on a predefined area threshold determined during model setup. The selection of this threshold is a subjective but critical process, as it directly influences model performance, computational efficiency, and spatial resolution (Pandey et al., 2019). A smaller threshold results in a greater number of sub-basins, improving spatial detail but substantially increasing computational demands. In this study, an area threshold of 15,000 hectares was applied (Chinnasamy and Sood, 2020), leading to the classification of the watershed into 21 sub-basins.

Subsequently, HRUs were defined by applying a 10% threshold for LULC, soil type, and slope, ensuring the retention of dominant hydrological characteristics while filtering out less significant spatial variations (Becker and Braun, 1999). This approach resulted in the generation of 180 unique HRUs, each representing a distinct combination of these three physiographic factors. The accurate delineation of sub-basins and HRUs is crucial for capturing spatial heterogeneity in hydrological processes, thereby enhancing the reliability of SWAT-based simulations.

The SWAT model was configured to simulate hydrological processes for the period 2000–2022, with the initial three years (2000–2002) designated as a warm-up period. This warm-up phase is essential for stabilizing key hydrological parameters such as soil water storage, groundwater levels, and aquifer recharge before generating model outputs.

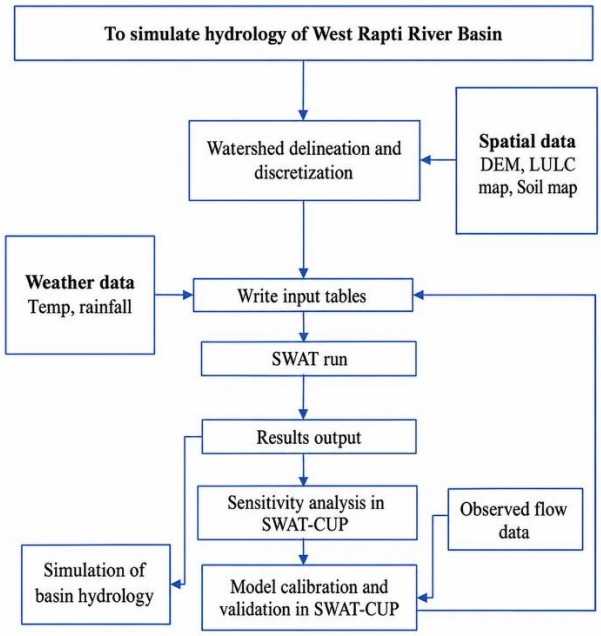

Figure 5, Workflow of research

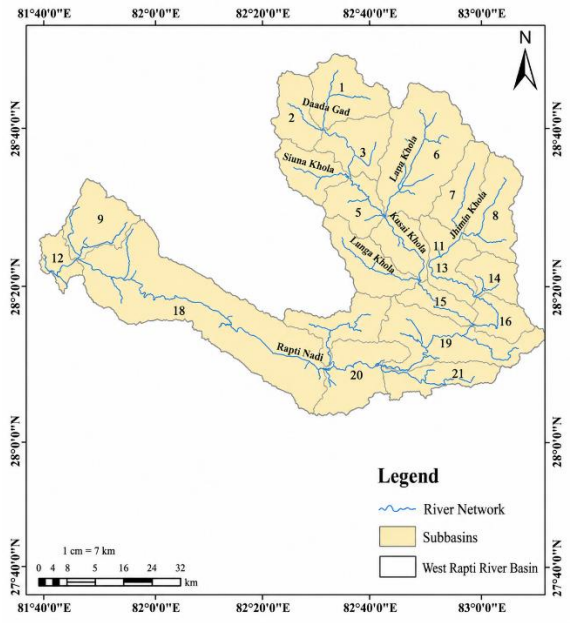

Figure 6, Sub-basins of the West Rapti River Basin

The inclusion of a warm-up period ensures that the model reaches a quasi-steady state, thereby minimizing initialization biases and improving the accuracy of subsequent hydrological simulations. Research by SWAT developers, including Douglas-Mankin et al. (2010), suggests that an optimal warm-up period typically ranges between one and three years, depending on the availability of input data and the complexity of the watershed. Given the availability of long-term observational data, this study adopted a three-year warm-up period (2000–2002) to enhance model reliability. Following this initialization stage, the model was calibrated for the years 2003–2011 and then validated for the years 2012–2020 using data on observed river discharges to evaluate its performance. Similarly, as there is observable sediment data up to

2015, the sediment was calibrated for 2003–2008 and validated for 2008–2014. By adjusting parameters to reflect observed hydrological responses, calibration and validation enhance the model's prediction power, making them essential phases in hydrological modeling.

Sensitivity analysis and model performance evaluation

The SWAT Calibration and Uncertainty Program (SWAT-CUP), a widely recognized tool for SWAT model calibration, was applied to adjust model parameters (Arnold et al., 2012). SWAT-CUP is extensively employed in hydrological research for model calibration, sensitivity analysis, and uncertainty analysis. In this study, the Sequential Uncertainty Fitting (SUFI-2) algorithm was applied to assess model uncertainty and optimize parameterization. The built-in Global Sensitivity Analysis tool in SWAT-CUP was employed for parameter sensitivity assessment and optimization. Global sensitivity analysis evaluates the collective impact of multiple parameters through multiple regression analysis. The degree of parameter sensitivity varied depending on watershed characteristics, model structure, hydrological state variables, and the spatial and temporal resolution of input data. The sensitivity analysis results were crucial in refining model calibration by optimizing parameter values to align with local hydrological conditions, thereby minimizing computational complexity and prediction uncertainty. Additionally, this process facilitated the evaluation of parameter interactions, range constraints, and spatial heterogeneity, contributing to improved model accuracy.

Initially, 23 parameters were shortlisted based on an extensive literature review, and the model simulation was executed for 400 iterations. From this analysis, the 11 most sensitive parameters were selected using statistical significance criteria, including p-values and t-test rankings. These parameters were then subjected to an additional 500 simulation runs with updated values for further refinement. Similarly, 18 sediment-sensitive parameters were studied to determine calibration and validation of sediment concentration in the model.

To evaluate model performance, two statistical indicators were employed: the coefficient of determination (R^2) and the Nash–Sutcliffe Efficiency (NSE). According to Moriasi et al. (2007), an R^2 value greater than 0.5 is generally considered acceptable, while an NSE value exceeding 0.5 indicates satisfactory model performance. These metrics provided quantitative validation of the model's predictive capability in simulating hydrological processes. The R^2 quantifies the proportion of variance in observed data that is explained by the model. The R^2 equation is given below in equation 2 (Michael and Jain, 2013):

$$R^2 = \frac{[\sum_{i=1}^{m}(q_{si}-\overline{q_s})(q_{oi}-\overline{q_o})]^2}{\sum_{i=1}^{m}(q_{si}-\overline{q_s})^2 \sum_{i=1}^{m}(q_{oi}-\overline{q_o})^2} \quad (2)$$

Where:

R^2 is the coefficient of determination, q_{si} is simulated flow, q_{oi} is observed flow, $\overline{q_s}$ and $\overline{q_o}$ are the average simulated and observed flow, respectively.

Similarly, the NSE quantifies the proportion of variance in observed data that is captured by the model, relative to the residual variance. The value of NSE can range from -∞ to 1.0, where values indicate poor model performance, and a value of 1 represents a perfect match between simulated and observed data. The NSE equation 3 (Nash and Sutcliffe, 1970) is given below:

$$NS = \frac{v_0 N - \sum_{i=1}^{m}(x_i-y_i)^2}{v_0 N} = 1 - \frac{\sum_{i=1}^{m}(x_i-y_i)^2}{\sum_{i=1}^{m}(x_i-\bar{x})^2} \quad (3)$$

Where the variance of the observed values is represented as v_0, m is the total number of data points to be analyzed, x_i is the observed value, y_i is the corresponding simulated value, and $\bar{x}$ is the average observed value for the study period.

Results and discussion

Model performance

The SWAT model was calibrated and validated for a monthly time scale in SWAT-SUFI2. Global sensitivity analysis prioritized sensitive parameters for flow as shown in Table 4. Table 4 presents the relative ranking of model parameters based on the student's t-stat and p-value. The ranking was assigned by prioritizing parameters with the highest absolute t-statistic, indicating greater sensitivity, and the lowest p-value, signifying higher statistical significance. The parameter exhibiting the largest t-statistic and the smallest p-value was designated as rank 1, reflecting its dominant influence on the model's performance, as shown in Table 4. The model parameter CN2 was a relatively more significant model parameter with a lower p-value at the catchment scale. The model parameter t-stat varied from -0.26 to 0.36. The outcome of the study identified that CN2 as most sensitive among 11 model parameters. Another sensitive parameter was base flow alpha factor (ALFA_BF) and Surface Runoff time lag (SURLAG).

Both R^2 and NSE were utilized to assess the SWAT model's performance in simulating flow during calibration and validation for the basin. The R^2 value, which ranges from 0 to 1, indicates the extent to which the model explains data variance. A value of 0 signifies no explanatory power, whereas a value of 1 represents a perfect fit (Arnold et al., 2012). Therefore, a higher R^2 value, approaching 1, implies a better model fit. According to Michael and Jain (2013), a model is considered to perform well if its indicator values exceed 0.5. NSE is a widely used metric in hydrological modeling to assess a model's ability to replicate observed data. According to Arnold et al. (2012), an NSE value greater than 0.75 indicates excellent performance, values between 0.36 and 0.75 suggest

satisfactory performance, and values below 0.36 reflect unsatisfactory performance. In this study, the R^2 and NSE values for calibration and validation in ARB and TRB remained above 0.75, signifying overall excellent model performance for monthly simulations.

The R^2 value for monthly flow during the calibration period was obtained as 0.95, accompanied by an NSE of 0.76, suggesting satisfactory model performance. However, during the validation period, the R^2 and NSE values dipped to 0.91 and 0.75, respectively. For flow calibration and validation in the basin, the model demonstrated excellent performance, with R^2 and NSE values consistently exceeding 0.75. The Figure 8 below shows the best fitted curves of flow out at sub-basin 18, i.e., Jalkundi station, during the calibration and validation period (Figure 7). The model simulated the flow pattern very well, and the hydrographs are in good agreement with the rainfall pattern. The scatter plot between observed flow and simulated flow also suggested that the model overestimated the base flow and underestimated the peak flows (Figure 8). Similar model performance is also evaluated for the SWAT model in Seti Gandaki Basin by KC et al. (2023), West Rapti Basin by Neupane and Pandey (2021), and Rapti River Basin by Kumari et al. (2024).

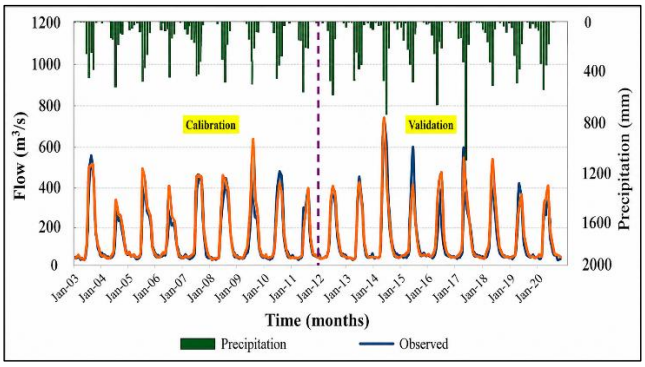

Figure 7, Calibration and validation curve

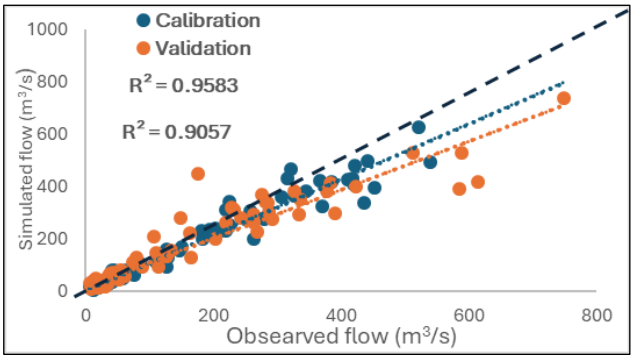

Figure 8, Scatter plot correlation

Table 4, Sensitive parameters for flow

Parameter	Description	Range	Fitting value	p-value	t-stat	Rank
R_CN2	Initial SCS runoff curve	67 to 90	68.72	0.72	0.36	1
R_ALFA_BF	Base flow alpha factor (days)	0.024 to 0.072	0.03	0.79	-0.26	2
A_SURLAG	Surface Runoff time lag (days)	0.05 to 24	23.40	0.80	0.24	3
R_SOL_AWC	Available Water Capacity (mm H2O/ mm soil)	0.0 to 1.0	0.675	0.84	-0.20	4
V_GWQMN	Threshold depth of water in the shallow aquifer required to start the return flow (mm H2 O)	0 to 2000	1450	0.93	0.08	5
V_LAT_TTIME	Lateral flow travel time (in days)	0 to 180	31.5	0.94	0.07	6
V_OV_N	Manning's "n" value for overflow flow	0.01 to 0.41	0.30	0.95	0.05	7
vV_SOL_Z	Depth from soil surface to bottom of layer (mm)	0 to 3500	3237.5	0.96	0.048	8
V_CH_K2	Effective hydraulic conductivity in main channel alluvium	0 to 150	71.25	0.97	0.043	9
V_GW_DELAY	Groundwater delay (days)	0 to 500	387.5	0.98	-0.022	10
R_CH_N2	Manning's "n" value for the main channel	0.01 to 0.3	0.0462	0.99	-0.012	11

Again, the calibration and validation for sediment involved the sensitive parameters as follows. Using the finalized sediment discharge rating equation, the sediment load (tonnes per day) was estimated. A daily data series was then generated, from which monthly sediment data were derived. This dataset was subsequently utilized for the calibration and validation of the SWAT model.

The R^2 value for monthly sediment during the calibration period was obtained as 0.65, accompanied by an NSE of 0.66, suggesting satisfactory model performance. However, during the validation period, the R^2 and NSE values dipped to 0.61 and 0.55, respectively.

SWAT model results

Hydrology and water balance

Spatial distribution of precipitation

Over the period of the 23-year run, the average annual precipitation distribution is estimated to be 1676.2 mm for the basin, with sub-basins 7 and 13 recording the highest amount (2617.7 mm) and sub-basins 10 and 11 experiencing the lowest (1092.2 mm) precipitation. 480.6 mm was the standard deviation of precipitation distribution among the sub-basins. Figure 11a shows

the spatial distribution of precipitation in the basin. Compared to the average precipitation that DHM observes, this simulated precipitation is somewhat exaggerated.

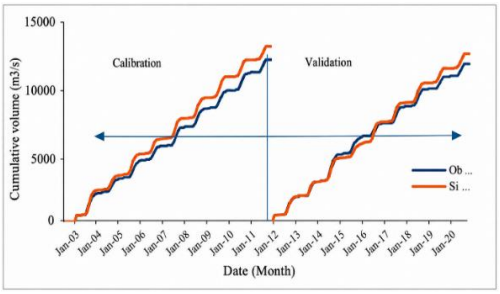

Figure 9, Cumulative flow volume curves

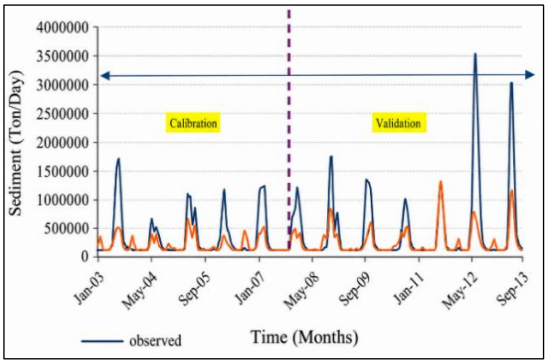

Figure 10, Calibration and validation curve for sediment

Table 5, Results of global sensitivity analysis and calibrated parameter values of the SWAT model obtained using the SUFI-2 algorithm in SWAT-CUP.

Parameter Name	Fitted Value	Min Value	Max Value	t-Stat	P-Value
V__CH_COV2.rte	0.408	0.36	1.00	-0.045048167	0.971340822
R__SOL_K(..).sol	-0.795	-0.94	1.22	-0.001688006	0.998925383
V__CH_K1.sub	7.75	0.00	10.00	0.056498201	0.964070325
R__SOL_BD(..).sol	-0.0495	-0.47	0.11	0.023819957	0.984838612
R__SLSUBBSN.hru	-0.30	-0.35	0.05	-0.052232961	0.966777656
V__OV_N.hru	2.38025	0.01	5.00	-0.121865253	0.922798843
V__CH_N1.sub	2.13225	-0.21	3.26	-0.041870080	0.973360239
V__CH_ERODMO(..).rte	0.435	-0.40	0.60	0.011318633	0.992794642
V__ADJ_PKR.bsn	1.5875	0.50	2.00	-0.008864086	0.994357096
R__SOL_Z(..).sol	0.38625	-0.03	0.42	0.000000000	1.000000000
R__USLE_K(..).sol	-0.2585	-0.19	0.27	0.033582860	0.978628519
R__HRU_SLP.hru	-0.12025	-0.15	0.02	-0.008472125	0.994606607
V__CH_S2.rte	0.537	0.24	0.68	0.023522648	0.985027778
V__PRF.bsn	0.5575	0.20	1.50	-0.065042844	0.958650684
R__CN2.mgt	-0.18975	-0.22	-0.11	0.059780293	0.961987921
V__CH_N2.rte	0.26375	0.01	0.30	0.034715605	0.977908231
V__CH_S1.sub	0.31725	-0.03	4.56	-0.084734476	0.946184908
R__USLE_P.mgt	-0.8225	-0.92	-0.66	0.033582860	0.978628519

The middle part of the river basin, which is primarily made up of the Jhimruk Khola watershed, experiences high precipitation. The denser forest cover and the upper Siwalik zone's tropical monsoonal regime may be attributed to the comparatively higher precipitation. The fact that this sub-basin is oriented in the windward zone of the Mahabharat range may be another factor. Because it is located in the semi-arid rain-shadow zone outside of the Mahabharat range, the western portion of the basin, or the downstream region, saw relatively less rainfall. At the same time, the leeward side of the Mahabharat Range and a few higher peaks cause less rainfall in the upstream portion of the West Rapti River, which is primarily in the districts of Rolpa and Salyan.

Spatial distribution of surface runoff

The average annual surface runoff was estimated as 573.4 mm in the model, with sub-basin 13 estimating the highest runoff (1180.1 mm) and sub-basin 11 estimating the lowest (276.2 mm). The standard deviation (284.7 mm) suggested variability in runoff distribution among the sub-basins of WRB. Figure 11b shows the spatial distribution of surface runoff in the basin.

Spatial distribution of water yield and evapotranspiration

With a low water output of 442 mm for sub-basin 10 and a high of 1845 mm for sub-basin 13, the average annual water yield in the basin was calculated to be 951.28 mm. Figure 11c shows the regional distribution of water yield in WRB. The Jhimruk Khola and downstream sub-basins were estimated to experience high evapotranspiration, with an average of 689.99 mm annually for the basin. The maximum was seen at sub-basin 19 and nearby sub-basins. These sub-basins, which have soil types of Je75-2a and Rd30-2b, are primarily composed of agricultural and mixed forest terrain contributed high evapotranspiration (Figure 11d).

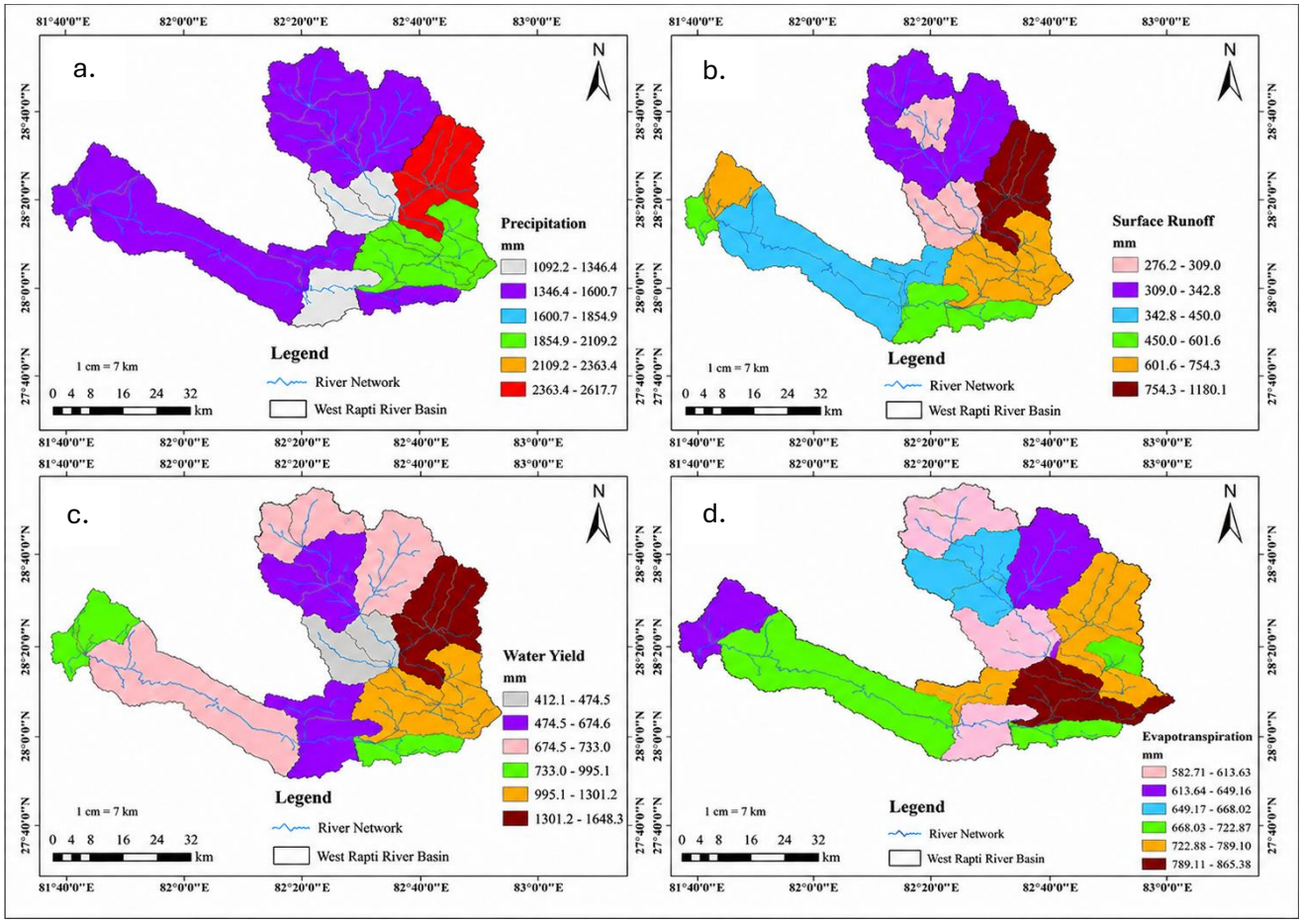

Figure 11, a. Precipitation and distribution map, b. Surface runoff and distribution map, c. Water yield distribution map, d. Evapotranspiration distribution map

Spatial distribution of sediment yield

The average annual sediment yield was determined to be 166 tonnes/ha by SWAT, with sub-basin 8 having the highest yield (468.05 tonnes/ha) and sub-basin 9 having the lowest (15.68 tonnes/ha) contribution. The standard deviation of sediment yield among the sub-basins was 32.06 tonnes/ha.

Figure 12 shows the spatial distribution of sediment yield in WRB. In the sub-basins, extremely high spatial diversity was noted. The Jhimruk Khola watershed region again attributed the highest yield of sediment to precipitation. This may suggest precipitation as a major erosion factor. This could also be due to the steeper topography of the Jhimruk Khola watershed. During the monsoon, surface runoff may potentially be the cause. Nonetheless, the Rapti River's downstream sub-basins made up a very small portion of the overall sediment budget.

Compared to the average sediment production of Nepalese river basins, this overall sediment yield or erosion rate is significantly higher (Sinha et al., 2019). Additionally, it exceeded the world average (Nepal et al., 2014).

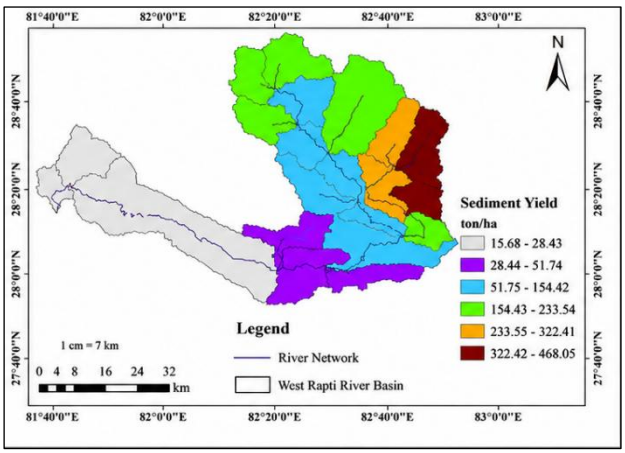

Figure 12, Sediment yield distribution map

Water balance in the West Rapti River basin

Out of the total precipitation that falls in the basin 55% flow as streamflow, 42% escape away as evapotranspiration. 55% contribute to streamflow. The remaining portion percolates to the aquifer (Figure 13).

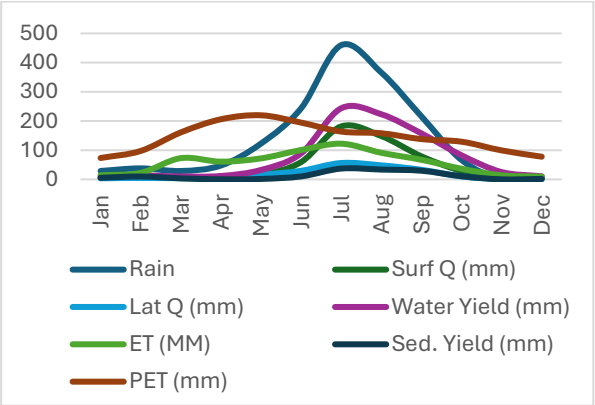

Figure 13, Water balance curves

Conclusion

This study successfully applied the SWAT model to simulate the baseline hydrology and water balance of Nepal's West Rapti River Basin, providing valuable insights into its hydrological processes and sediment dynamics. The model demonstrated strong predictive performance during calibration (R^2 = 0.95, NSE = 0.76) and validation (R^2 = 0.91, NSE = 0.75), accurately reproducing seasonal streamflow variability and sediment yield patterns. The most sensitive hydrological parameters were the curve number (CN2), baseflow recession coefficient (ALFA_BF), and surface runoff lag coefficient (SURLAG), emphasizing the combined influence of land use, soil characteristics, and runoff generation on basin hydrology. Long-term simulations (2000–2022) indicated a mean annual precipitation of 1,676 mm/yr, of which approximately 55% contributed to streamflow (951 mm/yr), while 42% was lost through evapotranspiration. Monsoon-driven surface runoff (573 mm/yr) dominated the hydrological regime, accounting for 68% of annual streamflow and approximately 85% of the annual sediment yield.

Sub-basin 8 was identified as the primary erosion hotspot, producing 468 t ha/yr because of its steep slopes (>40%) and highly erodible land use, highlighting the dominant role of topography in sediment generation. The spatial variability of evapotranspiration, surface runoff, and groundwater recharge reflected differences in land cover, soil properties, and terrain characteristics, resulting in distinct hydrological responses among forested, agricultural, and mixed land-use sub-basins. These findings demonstrate the basin's susceptibility to monsoon-driven hydrological extremes and land degradation, underscoring the need for targeted soil and water conservation measures in erosion-prone areas. The study provides a robust baseline for evaluating future climate and land-use change impacts and supports the development of sustainable watershed management strategies, including afforestation, soil conservation, and reservoir sedimentation control. Future research should integrate climate change projections and alternative land-use scenarios to assess long-term watershed resilience and guide adaptive water resource management.

Overall, the SWAT model proved to be an effective tool for quantifying the hydrology–sediment interactions of the West Rapti River Basin and provides a sound scientific basis for watershed planning and management in similar mountainous river basins.

References

Abdullah, M., and Al-Ansari, N. (2022). Missing rainfall data estimation: An approach to investigate different methods: Case study of Baghdad. Arabian Journal of Geosciences, 15(23), 1740. https://doi.org/10.1007/s12517-022-10995-6

Arnold, J. G., Moriasi, D. N., Gassman, P. W., Abbaspour, K. C., White, M. J., Srinivasan, R., Santhi, C., Harmel, R. D., Van Griensven, A., Van Liew, M. W., Kannan, N., and Jha, M. K. (2012). SWAT: Model use, calibration, and validation. Transactions of the ASABE, 55(4), 1491–1508. https://doi.org/10.13031/2013.42256

Arnold, J. G., Srinivasan, R., Muttiah, R. S., and Williams, J. R. (1998). Large-area hydrologic modeling and assessment: Part I. Model development. Journal of the American Water Resources Association, 34(1), 73–89. https://doi.org/10.1111/j.1752-1688.1998.tb05961.x

Ayele, G. T., Kuriqi, A., Jemberrie, M. A., Saia, S. M., Seka, A. M., Teshale, E. Z., Daba, M. H., Bhat, S. A., Demissie, S. S., Jeong, J., and Melesse, A. M. (2021). Sediment yield and reservoir sedimentation in highly dynamic watersheds: The case of Koga Reservoir, Ethiopia. Water, 13(23), 3374. https://doi.org/10.3390/w13233374

Basnet, N., Sitaula, S., Bohara, R., Bhattarai, S., Rawal, S., Uprety, M. P., Awasthi, M. P., Varol, M., Kayastha, S. P., and Pant, R. R. (2024). Hydro-chemical characteristics of Biring and Tangting rivers (Nepal) and evaluation of water quality for drinking and irrigation purposes. Environmental Research, 261, 119697. https://doi.org/10.1016/j.envres.2024.119697

Becker, A., and Braun, P. (1999). Disaggregation, aggregation and spatial scaling in hydrological modeling. Journal of Hydrology, 217(3), 239–252. https://doi.org/10.1016/S0022-1694(98)00291-1

Bekele, S., and Abate, B. (2020). Estimation of sediment yield using SWAT model: A case of Soke River Watershed, Ethiopia. International Journal of

Engineering Research and Technology, 9(12), 685–695.

Bhatta, B., Shrestha, S., Shrestha, P. K., Talchabhadel, R., 2019. Evaluation and application of a SWAT model to assess the climate change impact on the hydrology of the Himalayan River Basin. Catena, 181, 104082. https://doi.org/10.1016/j.catena.2019.104082

Bishwakarma, K., Wang, G., Zhang, F., Pant, R. R., Yuxuan, X., and Adhikari, S. (2024). Chemical weathering and CO2 consumption rates of the Koshi River Basin: Modeling and quantifying. Journal of Hydrology, 641, 131760. https://doi.org/10.1016/j.jhydrol.2024.131760

Bohara, R., Sitaula, S., Basnet, N., Awasthi, M. P., Rawal, S., Joshi, T. R., Byanju, R. M., and Pant, R. R. (2024). Hydrochemical characterization and water quality of perennial rivulets (Darchula), Sudurpashchim Province, Nepal. Tribhuvan University Journal, 39(2), 1–26. https://doi.org/10.3126/tuj.v39i2.72872

Chilagane, N. A., Kashaigili, J. J., Mutayoba, E., Lyimo, P., Munishi, P., Tam, C., and Burgess, N. (2021). Impact of land use and land cover changes on surface runoff and sediment yield in the Little Ruaha River Catchment. Open Journal of Modern Hydrology, 11(3), 54–74. https://doi.org/10.4236/ojmh.2021.113004

Chinnasamy, P., and Sood, A. (2020). Estimation of sediment load for Himalayan rivers: A case study of Kaligandaki in Nepal. Journal of Earth System Science, 129(1), 181. https://doi.org/10.1007/s12040-020-01437-6

de Oliveira Serrão, E. A., Silva, M. T., Ferreira, T. R., de Ataide, L. C. P., dos Santos, C. A., de Lima, A. M. M., da Silva, V. P. R., de Sousa, F. A. S., and Gomes, D. J. C. (2022). Impacts of land use and land cover changes on hydrological processes and sediment yield determined using the SWAT model. International Journal of Sediment Research, 37(1), 54–69. https://doi.org/10.1016/j.ijsrc.2021.04.002

Douglas-Mankin, K. R., Srinivasan, R., and Arnold, J. G. (2010). Soil and Water Assessment Tool (SWAT) model: Current developments and applications. Transactions of the ASABE, 53(5), 1423–1431. https://doi.org/10.13031/2013.34915

FAO (2002). FAO/UNESCO digital soil map of the world and derived soil properties (Land and Water Digital Media Series No. 1, Rev. 1). Food and Agriculture Organization of the United Nations, Rome.

FRTC (2022). Land cover of Nepal [Data set]. FRTC. https://doi.org/10.26066/RDS.1972729

KC, M., Aryal, I., Dhakal, N. R., and Marahatta, S. (2023). Application of SWAT hydrological model to simulate flow of the Seti-Gandaki Basin. Jalawaayu, 3(1). https://doi.org/10.3126/jalawaayu.v3i1.52060

Kumari, S., Singh, V., Suryavanshi, S., and Kumar, M. (2024). Application of the SWAT model for hydrological simulation of the Rapti River Basin. Journal of Experimental Agriculture International, 46 (6), 140-153. https://doi.org/10.9734/jeai/2024/v46i62466

Li, H., Yu, C., Qin, B., Li, Y., Jin, J., Luo, L., Wu, Z., Shi, K., and Zhu, G. (2022). Modeling the effects of climate change and land use/land cover change on sediment yield in a large reservoir basin in the East Asian monsoonal region. Water, 14(15), 1–19. https://doi.org/10.3390/w14152346

Liu, Y., and Jiang, H. (2019). Sediment yield modeling using the SWAT model: Case of the Changjiang River Basin. IOP Conference Series: Earth and Environmental Science, 234(1), 012031. https://doi.org/10.1088/1755-1315/234/1/012031

Michael, K. H., and Jain, M. (2013). Runoff and sediment modeling using SWAT in Gumera Catchment, Ethiopia. Open Journal of Modern Hydrology, 3(4), 196–205. https://doi.org/10.4236/ojmh.2013.34024

Moges, D., Moges, D. M., and Bhat, H. G. (2020). Watershed degradation and management practices in north-western highland Ethiopia. Environmental Monitoring and Assessment, 192(10), 664. https://doi.org/10.1007/s10661-020-08628-0

Moriasi, D. N., Arnold, J. G., Van Liew, M. W., Binger, R. L., Harmel, R. D., and Veith, T. (2007). Model evaluation guidelines for systematic quantification of accuracy in watershed simulations. Transactions of the ASABE, 50(3), 885–900. https://doi.org/10.13031/2013.23153

Nash, J. E., and Sutcliffe, J. V. (1970). River flow forecasting through conceptual models: Part I—A discussion of principles. Journal of Hydrology, 10(3), 282–290. https://doi.org/10.1016/0022-1694(70)90255-6

Nepal, J., Pant, R. R., Shrestha, S., Paudel, S., Bishwakarma, K., Awasthi, M. P., and Dhital, Y. P. (2024). Water balance estimation and runoff simulation of Chameliya Watershed, Nepal. Environmental Earth Sciences, 83(3), 117. https://doi.org/10.1007/s12665-024-11430-7

Nepal, S., Flügel, W.-A., and Shrestha, A. B. (2014). Upstream-downstream linkages of hydrological processes in the Himalayan region. Ecological Processes, 3(1), 19. https://doi.org/10.1186/s13717-014-0019-4

Neupane, S. N., and Pandey, A. (2021). Hydrological modeling of the West Rapti River Basin of Nepal using the SWAT model. In A. Pandey, S. Mishra, M. Kansal, R. Singh, and V. Singh (Eds.), Water management and water governance (Vol. 96, pp. XX–XX). Springer,

Cham. https://doi.org/10.1007/978-3-030-58051-3_19

Owens, P.N.(2020).Soil erosion and sediment dynamics in the Anthropocene: A review of human impacts during a period of rapid global environmental change. Journal of Soils and Sediments, 20(12), 4115-4143. https://doi.org/10.1007/s11368-020-02815-9

Pandey, V. P., Dhaubanjar, S., Bharati, L., and Thapa, B. R. (2019). Hydrological response of Chamelia Watershed in Mahakali Basin to climate change. Science of the Total Environment, 650, 365–383. https://doi.org/10.1016/j.scitotenv.2018.09.053

Pant, R. R., Varol, M., Phuyal, S., Bhattarai, S., Awasthi, M. P., Thakur, T. K., Bohara, R., and Afandi, G. E. (2025). How sand mining is shaping the Trishuli River in the Himalayas of South Asia. Earth Systems and Environment, 1–17. https://doi.org/10.1007/s41748-025-00569-3

Rahman, M. M., Harada, D., and Egashira, S. (2024). Sediment transport processes in the Sangu River Basin using a rainfall-sediment runoff model for sustainable river management. Proceedings of IAHS, 386, 109–114. https://doi.org/10.5194/piahs-386-109-2024

Ren,S., Zhang,B.,Wang, W.J.Yuan,Y.& Guo, C (2021). Sedimentation and its response to management strategies of the Three Georges River, Yangste River, China.Catena, https://doi.org/10.1016/j.catena.2020.105096

Schweizer, M., Dieterich, A., Corral Morillas, N., Dewald, C., Miksch, L., Nelson, S., Wick, A., Triebskorn, R., and Köhler, H. R. (2018). The importance of sediments in ecological quality assessment of stream headwaters: Embryotoxicity along the Nidda River and its tributaries in Central Hesse, Germany. Environmental Sciences, 30(1), 22 https://doi.org/10.1186/s12302-018-0150-4

Shi, X., Zhang, F., Lu, X., Wang, Z., Gong, T., Wang, G., and Zhang, H. (2018). Spatiotemporal variations of suspended sediment transport in the upstream and midstream of the Yarlung Tsangpo River (the upper Brahmaputra), China. Earth Surface Processes and Landforms, 43(2), 432–443. https://doi.org/10.1002/esp.4258

Shinde, V. M., Deshpande, P. K., and Kumthekar, M. B. (2013). Application of ASTER DEM in watershed management as flood zonation mapping in Koyana River of the Western Ghats. International Journal of Scientific and Engineering Research, 4(5), 297–301.

Sinha, R., Gupta, A., Mishra, K., Tripathi, S., Nepal, S., Wahid, S. M., and Swarnkar, S. (2019). Basin-scale hydrology and sediment dynamics of the Koshi River in the Himalayan foreland. Journal of Hydrology, 570, 156–166. https://doi.org/10.1016/j.jhydrol.2018.12.051

Srivastava, A., Deb, P., and Kumari, N. (2020). Multi-model approach to assess the dynamics of hydrologic components in a tropical ecosystem. Water Resources Management, 34, 327–341. https://doi.org/10.1007/s11269-019-02452-z

Subedi, S. R., Lamichhane, M., Dhungana, S., Chalise, B., Bhattarai, S., Chaulagain, U., and Khatiwada, R. (2024). Assessing the impact of climate change on streamflow in the Tamor River Basin, Nepal: An analysis using SWAT and CMIP6 scenarios. Discover Civil Engineering, 1, 135. https://doi.org/10.1007/s44290-024-00143-2

Thapa, B., Shrestha, R., Dhakal, P., and Thapa, B. S. (2005). Problems of Nepalese hydropower projects due to suspended sediments. Aquatic Ecosystem Health and Management, 8(3), 251–257. https://doi.org/10.1080/14634980500218241

Thomas, J., Joseph, S., Thrivikramji, K. P., and Arunkumar, K. S. (2014). Sensitivity of digital elevation models: The scenario from two tropical mountain river basins of the Western Ghats, India. Geoscience Frontiers, 5(6), 893–909. https://doi.org/10.1016/j.gsf.2013.12.008

Toma, M. B., Belete, M. D., and Ulsido, M. D. (2023). Hydrological components and sediment yield response to land use and land cover change in the Ajora-Woybo Watershed of Omo-Gibe Basin, Ethiopia. Air, Soil and Water Research, 16, 1–17. https://doi.org/10.1177/11786221221150186

Van Oost, K., Van Rompaey,A. Poesen, J.Grovers,G& Verstraeten,G.(2002).Evaluating an integrated approach to catchment management to reduce soil loss and sediment pollution through modeling. Soil Use and Manangement , 18(4)386-394. https://doi.org/10.1079/sum.2001.150

Vercruysse, K., Grabowski, R.C., & Rickson, R.J(2017). Suspended sediment transport dynamics in rivers: multi-scale drivers of temporal variation. Earth _ science Reviews, 166, 38-52. https://doi.org/10.1016/j.earscirev.2016.12.016